Title
THE INTERCALATION OF ETHIDIUM ION INTO DNA AND RNA OLIGONUCLEOTIDES

Author
Tinoco, I.

Publication Date
1983

Lawrence Berkeley Laboratory
UNIVERSITY OF CALIFORNIA

CHEMICAL BIODYNAMICS DIVISION

Submitted to Biopolymers

THE INTERCALATION OF ETHIDIUM ION INTO DNA AND RNA OLIGONUCLEOTIDES

Jeffrey W. Nelson and Ignacio Tinoco, Jr.

January 1983

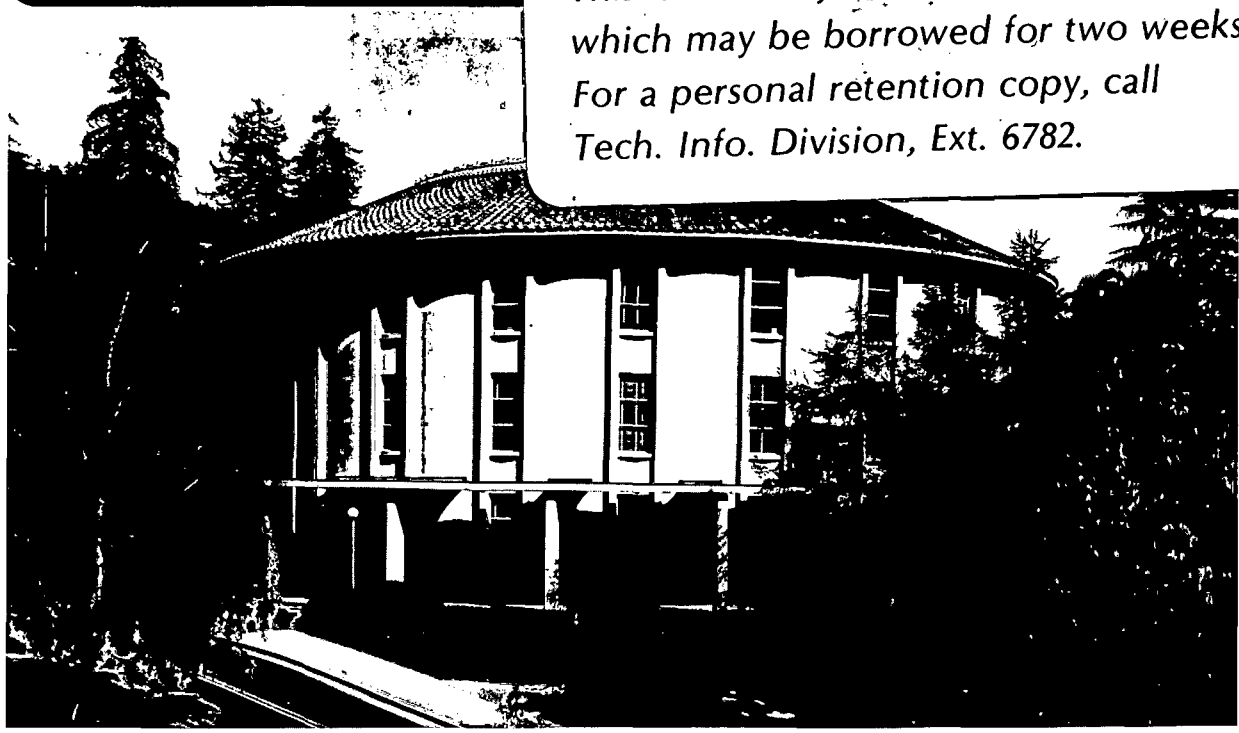

Prepared for the U.S. Department of Energy under Contract DE-AC03-76SF00098

DISCLAIMER

LBL-15506

THE INTERCALATION OF ETHIDIUM ION INTO DNA AND RNA OLIGONUCLEOTIDES

Jeffrey W. Nelson* and Ignacio Tinoco, Jr.

Department of Chemical Biodynamics
Lawrence Berkeley Laboratory
and
Department of Chemistry
University of California
Berkeley, California 94720

January 1983

*Present address: E.I. du Pont de Nemours & Co., Photo Products Dept., Experimental Station Laboratory, Wilmington, DE 19898.

This work was supported in part by the U.S. Department of Energy, Office of Energy Research under Contract No. DE-AC03-76SF00098 and Contract No. 03-82ER60090.000 and in part by National Health Grant GM 10840.

THE INTERCALATION OF ETHIDIUM ION INTO DNA AND RNA OLIGONUCLEOTIDES

Jeffrey W. Nelson and Ignacio Tinoco, Jr.

Indexing Phrases:

Ethidium binding to oligonucleotides

Sequence dependence of binding

Oligonucleotide binding properties

Intercalation

Synopsis

The thermodynamics of ethidium ion binding to the double strands formed by the ribo-oligonucleotides rCA_5G + rCU_5G and the analogous deoxyribo-oligonucleotides dCA_5G + dCT_5G were determined by monitoring the absorbance *vs.* temperature at 260 and 283 nm at several concentrations of oligonucleotides and ethidium bromide. A maximum of three ethidium ions bind to the oligonucleotides, which is consistent with intercalation and nearest-neighbor exclusion. For the ribo-oligonucleotide the binding sites were very unequivalent. Either two sites (assumed to be the intercalation sites at the two ends of the oligonucleotide) bind more strongly by a factor of 140 than the third site, or all sites are identical, but there is strong anticooperativity on binding (cooperativity parameter of 0.1). In sharp contrast, the binding to the same sequence (with thymine substituted for uracil) in the deoxyribo-oligonucleotide showed all sites equivalent and no cooperativity. For the ribo-oligonucleotides the enthalpy for ethidium binding is -14 kcal/mol. The equilibrium constants at 25°C depend on the model; either $K = 6 \times 10^5\ M^{-1}$ for the two strong sites ($4.3 \times 10^3\ M^{-1}$ for the weak site), or $K = 2.5 \times 10^5\ M^{-1}$ for the intrinsic constant of the anticooperative model. For the equivalent deoxyribo-oligonucleotide the enthalpy of binding is -9 kcal/mol and the equilibrium constant at 25°C is a factor of ten smaller ($K = 2.5 \times 10^4\ M^{-1}$).

INTRODUCTION

A large number of molecules that cause frameshift mutations intercalate between the base pairs of nucleic acids. Streisinger et al. (1) proposed a model in which the mutagen promotes frameshift mutations via the stabilization of a bulge after strand breakage in DNA. This bulge is then locked into the sequence when the break is repaired. Ethidium bromide has been shown to be a frameshift mutagen in the Ames test, and a strong correlation was found between frameshift mutagenicity and chemical carcinogenicity (2).

Several factors make ethidium ion an ideal probe. It intercalates with a large binding constant, making it possible to prepare samples in which essentially all of the ethidium is bound. Intercalation is accompanied by a large shift in the visible absorption band at 480 nm to longer wavelengths (3,4). Also, the fluorescence is enhanced greatly upon intercalation (5). Ethidium ion dimerizes in solution; however the extent of aggregation is small compared to intercalators such as the acridines (6,7). Ethidium ion binds to single-stranded nucleic acids (8), but the binding is very much weaker than intercalation in double-stranded nucleic acids (4).

Studies of ethidium ion binding to DNA have demonstrated that binding occurs with nearest-neighbor exclusion, and with very little cooperativity (9). Overall binding constants may be obtained by this procedure; however sequence-specific properties are inaccessible due to the randomness of the DNA sequence.

Studies carried out on dinucleoside phosphates and dinucleotides have shown that there is a preference for ethidium binding to double-stranded sequences in the order pyrimidine-purine > purine-purine > purine-pyrimidine (7,10,11,12). However, the dinucleotides form very unstable mini-double helices by themselves, as indicated by the equilibrium constant for double

strand formation from the self-complementary dinucleotide pdG-dC being on the order of 10 M^{-1} (13,14). Dinucleotides composed of only A•T or A•U base pairs have equilibrium constants which are too small to measure. Thus the sequence specificity found in these studies is complicated by the fact that the stability of the double strand in the absence of ethidium bromide is not well-known.

Ethidium ion forms complexes with the double helix formed by the trinucleoside diphosphate rCpUpG by intercalating between the two C•G base pairs, bulging the two uracils into solution (15). There is also a complex formed between a mixture of rGpUpG, rCpC, and ethidium, wherein the two C•G base pairs are formed with the uracil bulged into solution (15). The equilibrium constants for the complex of ethidium with rCpG and with rCpUpG were measured at 0°C to be 100 x 10^6 and 1 x 10^6 M^{-2}, respectively (16). Thus, the bulged uracils destabilize the structure significantly. The equilibrium constant for the complex formed by rGpUpG, rCpC, and ethidium was less than 10^5 (16). Polymer studies on the double strands poly(I)•poly(C,A), showed that the equilibrium constant of ethidium binding to the site with the A•I mismatch is about 20 times greater than that for binding to the normal base pairs (17). This indicates that ethidium ion might relieve some of the destabilizing effect of the mismatched bases.

Oligonucleotides allow studies of sequence effects and have the advantage that the properties of the double strands in the absence of ethidium are known (18). Potentially, oligonucleotide studies can be used to determine the destabilizing effect of a bulged base, and the extent to which ethidium binding relieves this strain.

In this paper, we report the results on the binding of ethidium bromide to the double strands formed by the oligonucleotides rCA_5G + rCU_5G and dCA_5G +

dCT_5G. The extent of ethidium binding is measured by monitoring the large change in absorbance in the UV band of ethidium at 283 nm. Fortunately, at this wavelength, the double-stranded oligonucleotides absorb to the same extent as the single strands. A statistical model is described wherein the ethidium cation can bind between any combination of base pairs within the nearest-neighbor limit. A more detailed discussion of the results has been written elsewhere (19).

EXPERIMENTAL

The synthesis and characterization of the oligonucleotides rCA_5G, rCU_5G, dCA_5G and dCT_5G were described previously (20). Ethidium bromide was purchased from Sigma; to remove any ethanol present, the ethidium bromide was lyophilized twice with double-distilled water prior to use.

The buffer used throughout this study consisted of 0.2M NaCl, 0.01M sodium phosphate buffer, pH = 7, and 0.1mM EDTA. Samples were prepared by adding small amounts of concentrated stock solutions of the oligonucleotides and ethidium bromide to the buffer. The buffer was degassed by purging with helium for three to four minutes prior to preparing the samples.

Samples of the ribo-oligonucleotides were made up with nominal concentrations of 50μM, 25μM, and 12μM, with ethidium:strand ratios of approximately 0, 0.1, 0.2, 0.5, 1, 2, and 3. One sample contained 50μM strands and a 4:1 ratio of ethidium:strands. Eppendorf 1.5ml polypropylene micro centrifuge tubes were used to prepare the samples. Tubes were pre-treated by rinsing with an ethidium bromide solution to avoid adsorption of ethidium from the samples. The actual concentrations were determined using the absorbances at 50°C, where the oligonucleotides are single-stranded, and the ethidium is unbound. When the melting curve was not finished by 50°C, the absorbances of single strands and free ethidium at 50°C were determined by extrapolating the absorbances at higher temperatures.

The deoxyribo-oligonucleotide samples were made at a concentration of about 40 M, with ethidium:strand ratios of about 0.4, 0.6, and 0.8. Because ethidium does not bind as strongly to the deoxyribo-oligonucleotides, studies were impractical at ethidium:strand ratios greater than 1.0 (see results).

MEASURING MELTING CURVES

Melting curves were obtained using a Gilford Model 250 UV-VIS spectrophotometer, with a Gilford Model 2527 thermoprogrammer. The cuvettes were Teflon stoppered with path lengths of 0.1, 0.2, 0.5 or 1 cm. Data were obtained concurrently at 260 and 283 nm using a Gilford Model 2530 wavelength scanner. The data were collected by a Commodore PET Model 2001 microcomputer interfaced to the instrument and were later transmitted to a VAX 11/780 computer, where the analysis was done. The melting data were interpolated to every 1°C, since analysis of the data requires knowing the absorbances at both 260 and 283 nm at the same temperature (see below). The temperature range for the oligonucleotides was generally 0°C to 70°C. The sample was returned to 0°C after attaining the high temperature to check for evaporation; changes in absorbance were less than 1%. Spectra were taken on the Gilford Model 250 spectrophotometer modified to allow the PET computer to control the wavelength.

Samples for melting curves of ethidium bromide in buffer were prepared in unstoppered cuvettes, which were covered with silicon oil (Dow Corning 200 Fluid, 20cS viscosity) to ensure that evaporation was negligible. No detectable amount of ethidium went into the oil. The melting curves for the ethidium bromide were taken from 0°C to 90°C. Spectra of ethidium were taken at 0°C, 25°C, and 50°C in stoppered cuvettes.

ANALYZING MELTING CURVES

From the melting curves, we want to measure f_b, the fraction of ethidium ions bound, and f_h, the fraction of strands in double helices (with or without ethidium ions bound). We can obtain this information from melting curves measured at two wavelengths, 260 and 283 nm. If we assume that the absorbance of an intercalated ethidium ion is the same at all of the intercalation sites, and that the absorbance of the ethidium is independent of the number of ethidium ions bound, then we can write expressions for the absorbance at 260 and 283 nm, A_{260} and A_{283}, as follows:

$$A_{260}/\ell = C_t[f_h\varepsilon_{h,260} + (1 - f_h)\,\varepsilon_{s,260}] + C_d[f_b\varepsilon_{b,260} + (1 - f_b)\,\varepsilon_{f,260}] \quad (1)$$

$$A_{283}/\ell = C_t[f_h\varepsilon_{h,283} + (1 - f_h)\varepsilon_{s,283}] + C_d[f_b\varepsilon_{b,283} + (1 - f_b)\varepsilon_{f,283}] \quad (2)$$

Here, ℓ is the path length in cm, C_t is the total concentration of each non-self-complementary single strand, C_d is the total ethidium concentration, $\varepsilon_{h,260}$ is the extinction coefficient at 260 nm of the double helices with no ethidium bound, $\varepsilon_{s,260}$ is the extinction coefficient at 260 nm of the single strands, $\varepsilon_{b,260}$ is the extinction coefficient at 260 nm of a bound ethidium ion, and $\varepsilon_{f,260}$ is the extinction coefficient at 260 nm of the free ethidium ion, with analogous definitions for 283 nm.

Once the extinction coefficients are known, Equations (1) and (2) can be solved simultaneously to determine the values for f_h and f_b. In general, the extinction coefficients will depend on the temperature.

In the oligonucleotides studied here, the absorbance of the double strands at 283 nm is nearly the same as that of the single strands, namely $\varepsilon_{h,283} \cong \varepsilon_{s,283}$. In this case, the value of f_b can be determined from Equation (2) alone:

$$A_{283}/\ell = C_t\varepsilon_{s,283} + C_d[f_b\varepsilon_{b,283} + (1 - f_b)\varepsilon_{f,283}] \qquad (3)$$

Both methods yielded the same values for f_b within 0.01.

THEORY

DESCRIPTION OF THE MODEL

Two different statistical models were used to describe the binding of ethidium ions to the double helices formed by rCA_5G + rCU_5G or dCA_5G + dCT_5G. One model assumes that the two terminal binding sites, $\overset{C-A}{\underset{G-U}{}}$ and $\overset{A-G}{\underset{U-C}{}}$, are stronger than the internal $\overset{A-A}{\underset{U-U}{}}$ binding sites by a factor τ. $\tau = 1$ corresponds to the model with all binding sites equal. This model was chosen because NMR experiments indicate ethidium binds preferentially at these sites (A. Pardi and K. M. Morden, unpublished data). The other model assumes that there is cooperativity between binding sites, where the parameter ω describes the effect of one bound ethidium ion on the adjacent next nearest neighbor binding site.

For both models, we assume that binding occurs only <u>via</u> intercalation between base pairs in the double helix; no binding is allowed on the ends of the helix, or on the single strands. Also, we assume that binding occurs with nearest-neighbor exclusion: binding an ethidium ion between two base pairs makes the adjacent site unavailable for binding another ethidium ion.

The model will be developed using the assumption that the two terminal binding sites are τ times stronger than the interior sites, with no cooperativity. As will be explained, the theory is very easily modified to accomodate alternative models.

We denote the equilibrium constant for double-helix formation K_h:

$$rCA_5G + rCU_5G \overset{K_h}{\rightleftharpoons} \overset{rC-A-A-A-A-A-G}{\underset{G-U-U-U-U-U-Cr}{}} \qquad (4)$$

The equilibrium constant for binding ethidium to any of the interior sites is denoted K_d:

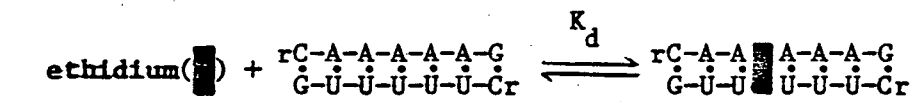

(5)

The equilibrium constant for binding ethidium to the terminal binding sites is denoted τK_d. Hence the terminal sites are τ times stronger than the interior sites. Nearest-neighbor exclusion allows only three ethidium ions to bind per double helix. Table I shows some of the possible arrangements of binding one, two, or three ethidium ions. There are 6 ways to bind one ethidium ion, 10 ways to bind two, and 4 ways to bind three.

If C_s is the equilibrium concentration of the single strands, and C_f is the concentration of the free ethidium, then the concentration of double helices with one ethidium ion bound to a specific interior site is $K_h K_d C_f C_s^2$. The concentration of double helices with one ethidium bound to a specific terminal site is $\tau K_h K_d C_f C_s^2$. If we assign $S = K_d C_f$, we can write the concentration of double helices with i ethidium ions bound in a specific arrangement as $\tau^j K_h S^i C_s^2$ where j terminal sites are filled, j = 0 to 2.

To develop the statistical approach, we define the statistical weight of each species as shown in Table I, namely $\tau^j K_h S^i$ for a double strand with i ethidium ions bound, with j in terminal binding sites. The single strands are defined as the reference state, and hence have a statistical weight of 1. In order to simplify the calculation of the sum of statistical weights, we will define statistical factors g_i for the double helices with i ethidium ions bound. Here, i varies from 0 to n, where n is the maximum number of ethidium ions that can bind. The factor g_i describes the number of ways i ethidium ions can bind, and their relative strengths. For example, there are six ways one ethidium ion can bind to these double strands: two ways to a terminal

binding site and four ways to an interior site. Thus, $g_1 = 2\tau + 4$. Table I shows the number of ways to bind 0 to 3 ethidium ions, the statistical weights, and the statistical factors g_i. As shown, $g_0 = 1$, $g_1 = 2\tau + 4$, $g_2 = \tau^2 + 6\tau + 3$, and $g_3 = 2\tau^2 + 2\tau$.

The partition function describing the double-helical species with or without ethidium ions bound is defined as Q:

$$Q = \sum_{i=0}^{n} g_i K_h S^i \tag{6}$$

If the total concentrations of the non-self-complementary single strands are equal, the total concentration of double helical species, C_h, is obtained from the partition function by:

$$f_h = C_h/C_t = \frac{1 + 2QC_t - \sqrt{1 + 4QC_t}}{2QC_t} \tag{7}$$

The expression for the total amount of ethidium bound can be written as the fraction of ethidium bound, $f_b = C_b/C_d$:

$$f_b = C_b/C_d = \left(\frac{f_h C_t}{C_d} \right) \sum_{i=1}^{n} iP_i \tag{8}$$

$$P_i = C_i/C_h = g_i K_h S^i/Q \tag{9}$$

We use standard numerical solution techniques to relate f_b and f_h to K_h, K_d, C_t, C_d and τ.

The previous development may be performed for a number of different models. The only difference is the form of the statistical factors g_i. We can assume a model in which there is cooperativity between ethidium binding sites by defining a cooperativity parameter ω as the equilibrium constant for:

(10)

Thus, $\omega > 1$ means a bound ethidium enhances binding at the next available site

(cooperative binding), and $\omega < 1$ means a bound ethidium reduces binding at the next available site (anticooperative binding). The statistical weights of the species with two or more ethidium ions bound are then multiplied by ω for each time that two bound ethidium ions are two base pairs apart. The values for the statistical factors for this model are easily shown to be: $g_0 = 1$, $g_1 = 6$, $g_2 = 4\omega + 6$, and $g_3 = 2\omega^2 + 2\omega$.

FITTING THE MODEL PARAMETERS TO EXPERIMENTAL RESULTS

After experimentally determining f_b, the fraction of ethidium bound to double helices, we need a procedure to determine the best values of K_d and τ to fit the data. We used the following method.

The first step is to pick an arbitrary value for τ. In general, $\tau = \exp(\Delta S^\circ_\tau/R - \Delta H^\circ_\tau/RT)$, where ΔH°_τ and ΔS°_τ are the differences of the enthalpy and entropy between the terminal and interior binding sites. Usually, the difference will be attributed entirely to the entropy, making τ independent of temperature.

Using this fixed value for τ, Equation (8) may be solved numerically for K_d, using the experimental value of f_b at any particular temperature. Several melting curves at different strand concentrations and ethidium:strand ratios are fit simultaneously. The values of ΔH°_d and ΔS°_d are obtained by linear regression analysis of the plot of $\ell n(K_d)$ vs. $1/T$. We may now calculate theoretical values for f_b for each point in the melting curves. The goodness of fit can be evaluated both by the linear correlation coefficient, r, from the linear regression analysis, or by the total reduced chi-squared determined for all the melting curves, $\chi^2 = (f_{d,calc} - f_{d,expt})^2/(N - 2)$ where there are N data points from all the melting curves (21). The reduced chi-squared is the more sensitive parameter, although both criteria resulted in the same best values for τ.

RESULTS

OPTICAL PROPERTIES OF ETHIDIUM BROMIDE IN THE UV

Most of the work on the binding of ethidium bromide to nucleic acids has been done by monitoring the absorbance of ethidium bromide in the visible band near 480 nm. This has the advantage that the absorbance of the nucleic acids does not interfere with the measurement, allowing the use of a large excess of nucleic acids. However, in this work, we carried out the studies in the UV. Since the extinction coefficient of ethidium bromide is about 10 times greater at 283 vs. 480 nm, this allowed us to work at ethidium:strand ratios of 0.1 to 3.

A range of extinction coefficients for ethidium bromide at 480 nm have been reported (in terms of M^{-1} cm^{-1}): 5.6×10^3 (4), 5.45×10^3 (22), 5.9×10^3 (23), 5.85×10^3 (9), and 5.86×10^3 (7). We used an average value of $(5.8 \pm 0.2) \times 10^3$ M^{-1} cm^{-1}.

Ethidium bromide forms dimers at moderate concentrations, which causes a shift in the maximum absorbance to wavelengths greater than 480 nm (6). The equilibrium constant at 25°C for this dimerization was found to be 70 M^{-1} in 0.1M NaCl by NMR (7). At the most concentrated solution of ethidium bromide used in this study, 0.2mM, less than 3% of the ethidium was dimerized, and hence was considered negligible. Indeed, there was no significant departure from Beer's law at 260 or 283 nm for ethidium bromide up to 1mM concentration.

The absorption spectrum in the range of 220 to 380 nm of ethidium bromide depends on temperature. The wavelength of the maximum absorbance was found to be 284 nm at 0°C, 285 nm at 25°C, and 286 nm at 50°C. The absorption spectra at any temperature were superimposable between 260 and 380 nm over the concentration range of 0.01mM to 0.2mM. The spectra deviated with concentration below 250 nm, with higher concentrations having larger absorbances.

The extinction coefficients at 283 nm and 260 nm at 25°C were obtained by comparing the absorbance of a dilute solution (20μM) at 480, 283 and 260 nm: $\varepsilon_{283} = 5.6 \times 10^4$ and $\varepsilon_{260} = 1.74 \times 10^4$. The extinction coefficient at 260 nm varied linearly with temperature and did not depend on concentration. It fit well to the equation $\varepsilon_{260}(T) = 1.7 \times 10^4 - 25.5(T - 50°C)$ (M^{-1} cm^{-1}). At 283 nm, the extinction coefficients depend on concentration. Absorbances measured from 0°C to 90°C are shown in Figure 1 for three ethidium concentrations. The change with concentration is not large, only about 3% at 0°C, and negligible above 50°C. The melting curves were fit very well by the empirical equation $\varepsilon_{283}(T)/\varepsilon_{283}(90°C) = 1 - 1.45 \times 10^{-3}(T - 90°C) + (4.9 \times 10^{-6}\sqrt{\text{concentration}} + 8.6 \times 10^{-9})(T - 90°C)^3$. The dependence of these equations on the square root of the concentration is an empirical relation that fits the data; no theoretical motivation was involved. The curves calculated using this equation are also shown in Figure 1. $\varepsilon_{283}(90°C)$ was found to be 5.1×10^4. All of the extinction coefficients are shown in Table II.

OLIGONUCLEOTIDE OPTICAL PROPERTIES

The extinction coefficients for the single-strand mixtures of rCA_5G + rCU_5G and dCA_5G + dCT_5G are readily determined by melting the single strands separately. At 283 nm, the extinction coefficients of the ribo-oligonucleotides were linear with temperature: $\varepsilon_{283}(T) = 4.17 \times 10^4 - 10.4(T - 50°C)$. The slope contributes only a 1% change between 0°C and 50°C. At 260 nm, the extinction coefficient of the ribo-oligonucleotides shows significant curvature, and is fit well to the third order equation: $\varepsilon_{260}(T) = 1.40 \times 10^5 + 190(T - 50°C) - 2.35(T - 50°C)^2 - 0.0237(T - 50°C)^3$. The fit by a second order expression was significantly worse.

The deoxyribo-oligonucleotide single strands are characterized by a linear extinction coefficient at 283 nm, $\varepsilon_{283} = 5.4 \times 10^4 + 40(T - 50°C)$. At

260 nm, the curve is also linear, $\varepsilon_{260}(T) = 1.41 \times 10^5 + 170(T - 50°C)$.

The fitting of the extinction coefficients of the double strands is difficult because the oligonucleotides form only moderately stable double strands. The absorbances of the double strands are temperature dependent (18,24,25); and the fact that the double strands aggregate causes the extinction coefficient of the double strands to depend on concentration (18).

The slope of the extinction coefficients at 260 nm for the double strands was determined from melting curves taken at a strand concentration of 1mM. For the ribo-oligonucleotides, $\varepsilon_{260}(T) = \varepsilon_{260}(0°C) + 240(T)$, with $\varepsilon_{260}(0°C)$ varying from 1.13×10^5 at 50μM to 1.15×10^5 at 12μM strand concentration. The deoxyribo-oligonucleotides were studied only at a strand concentration of 40μM: $\varepsilon_{260}(T) = 1.14 \times 10^5 + 150(T)$.

For both the oligonucleotide mixtures $rCA_5G + rCU_5G$ and $dCA_5G + dCT_5G$, the absorbance at 283 nm changes very little upon melting the double strands to single strands, making the determination of the double-strand extinction coefficients more straightforward. For the double-stranded ribo-oligonucleotides, $\varepsilon_{283} = 4.21 \times 10^4$, and for the deoxyribo-oligonucleotides, $\varepsilon_{283} = 5.25 \times 10^4$. Both extinction coefficients were independent of temperature within experimental error. Because the double strands and single strands absorb nearly the same, the determination of the fraction ethidium bound, f_b, is essentially determined at 283 nm only, using Equation (3). The extinction coefficients are included in Table II.

BINDING OF ETHIDIUM TO $rCA_5G + rCU_5G$

By monitoring the absorbance at 260 and 283 nm from low to high temperatures, we can monitor the fraction double strands and the fraction ethidium bound, as described in the theory section. Since the melting of the

double strands is nearly isosbestic at 283 nm, this wavelength monitors the state of ethidium binding. Conversely, 260 nm monitors mostly the double-strand to single-strand transition. The melting curves at 260 and 283 nm at a strand concentration of about 50μM at a range of ethidium:strand ratios are shown in Figure 2. The curves at 283 nm exhibit quite clearly the sigmoidal behavior characteristic of a cooperative transition at low ratios of ethidium:strand.

Since the leveling off of the curves at low temperature and low ethidium:strand ratios clearly indicates that the ethidium is fully bound, we can use the curve at low temperature to determine the extinction coefficient of the bound ethidium. The extinction coefficient thus determined is $\varepsilon_{283}(T) = 2.0 \times 10^4 + 50(T)$. The value for the extinction coefficient of bound ethidium is only 35% of that for free ethidium at 283 nm. The best fit for the curve at low ethidium:strand ratios varied for individual melting curves by about 10%. However, this is a small effect, considering the magnitude of the change.

The melting curves at 260 nm are more difficult to interpret; for these oligonucleotides the single-strand to double-strand transition is not fully over at 0°C in the absence of ethidium. Thus the determination of the extinction coefficient of bound ethidium is only an estimate: $\varepsilon_{260}(T) = 9.1 \times 10^3 - 15(T)$. Thus, the extinction coefficient of bound ethidium decreases by about 50% at 260 nm. However, since the extinction coefficient of the oligonucleotides at 260 nm is much larger than that of ethidium, the effect of ethidium binding on the absorbance is not as large as it is at 283 nm. These extinction coefficients are included in Table II.

Since the melting of the double strands to single strands is not completely isosbestic at 283 nm, the fraction double strands and ethidium

bound were calculated by using Equations (1) and (2). However, the approximation that the melting of the strands is isosbestic changes the fraction of ethidium bound [from Equation (3)] by less than 1%.

The stabilization of the double strands by ethidium binding is shown in Figure 3, which shows the fraction double strands in the absence and presence of a 1:1 ratio of ethidium bromide. Also shown is the fraction ethidium bound. Several features are apparent from this figure.

The melting of the double strands in the presence of ethidium is shifted to higher temperatures and is broadened significantly relative to the strands alone. The ethidium binding curve occurs at higher temperatures and is sharper relative to the strands in the mixture. For example, at around 33°C, when the double strands in the mixture are about half-formed, essentially no double strands are formed in the absence of ethidium. Furthermore, about 70% of the ethidium ions are bound to the double strands. Thus, essentially every double strand has at least one intercalated ethidium ion with an average of about 1.4 ethidium ions bound per double strand. This binding of multiple ethidium ions explains why the ethidium binding curve is sharper. The ethidium is nearly fully bound well before all of the double strands are formed. The last double strands must form without as much stabilization from the ethidium ions.

Further qualitative results may be derived by considering the behavior of ethidium binding at different ratios of ethidium:strand. Figure 4 shows the melting curves at ethidium:strand ratios of approximately 0.5, 1, 2, 3, and 4, at a constant strand concentration of 50μM. The binding curves at ethidium:strand ratios of 0.5 or 1 show that all of the ethidium is bound between 0°C and abput 15°C. The second ethidium ion also binds strongly, indicated by the fact that two ethidium ions are bound at 0°C at an

ethidium:strand ratio of 2.12. The third ethidium ion binds less strongly, since at an ethidium:strand ratio of 3.16 at 0°C, an average of only about 2.6 ethidium ions are bound per double strand. Figure 4 also shows very clearly that when four ethidium ions are present, only three bind. This confirms the assertion that ethidium binds with nearest-neighbor exclusion.

The best values for the model parameters K_d and τ were determined as described in the theory section. The analysis was performed on two sets of melting curves. Nine melting curves had ethidium:strand ratios of approximately 0.08:1; 0.18:1, 0.5:1 and 1.0:1, with total strand concentrations of approximately 12, 25 and 50μM. In addition, six melting curves were analyzed with ethidium:strand ratios of approximately 1.0:1, 2.1:1 and 3.2:1, with total strand concentrations of approximately 12 and 50μM. In both cases, the data were analyzed between f_b = 0.2 and 0.8, where the accuracy is the greatest. The values used for the thermodynamics of double-strand formation were ΔH_h° = -43 kcal/mol and ΔS_h° = -128 e.u. (18).

For the model which assumes that the two terminal binding sites are τ times stronger than the interior sites, the two sets of melting curves gave essentially the same results. In the data at high ethidium:strand ratios (1:1 to 3:1), the best fit occurred with τ = 140, with ΔH_d° = -11 kcal/mol, and τK_d = 6 x 10^5 (χ^2 = 1.7 x 10^{-4}, R = 0.995). The fit was very sensitive to the value of τ; changing τ by a factor of two more than doubled the value of the χ^2, and changed the enthalpy of ethidium binding by about 1.5 kcal/mol and the value of τK_d by about 15%. The fit for the data at low ethidium:strand ratios (1:1 or less) was much less sensitive to the value of τ, however the values of ΔH_d° and τK_d were also not sensitive to the value of τ. For example, for values of τ between 40 and 200, the value of χ^2 changed less than 14% from the lowest value of 1.3 x 10^{-4}. Over the same range of τ, the value of ΔH_d° varied

from -14.2 to -14.0 kcal/mol, and the value τK_d varied from 5.6×10^5 to 6.4×10^5. Presumably, at low ethidium:strand ratios, only the two strong terminal sites are significantly filled, and hence the fit is not influenced greatly by the properties of the weaker interior sites. This suggests that the properties of the stronger terminal binding sites are more accurately determined by the data at low ethidium:strand ratios, and the relative strengths of the terminal and interior sites are best determined by the data at high ethidium:strand ratios, where the weaker interior sites become important.

In the above analyses, we have assumed that the enthalpy of ethidium binding to the two types of sites were the same. This is equivalent to making τ independent of temperature, since $\tau = \exp(-\Delta H^\circ_\tau/RT + \Delta S^\circ_\tau/R)$ where ΔH°_τ and ΔS°_τ are the differences in the enthalpy and entropy between the terminal and interior sites. The fact that the data at high ethidium:strand ratios result in a more positive enthalpy of ethidium binding suggests that the interior sites have a more positive enthalpy, since the contribution of the interior binding sites is greater at higher ethidium:strand ratios. However, it would be inappropriate to attempt to quantitate the difference at this time.

Errors in the thermodynamics of the single-strand to double-strand transition can also contribute to the errors of the determination of the ethidium binding constants. Changing the enthalpy of double-strand formation by 10% changes the enthalpy of ethidium binding by about 2 kcal/mol, and changes the ethidium binding constant about 10%. Considering this, and the difference in enthalpy determined by the low and high ethidium:strand ratios, the error in the determination of the enthalpy of ethidium binding to the terminal site is probably less than 4 kcal/mol, and the equilibrium constant is probably good to about 15%. The results are shown in Table III.

In addition to the model which assumes that the two terminal binding sites are stronger than the interior sites, we tested a model which assumed that the binding of ethidium is cooperative, namely that a bound ethidium ion affects the next available binding site. The best fit indicated anti-cooperativity (ω = 0.1), and the fit to the data at both low and high ethidium:strand ratios was quite sensitive to the value of the cooperativity parameter, ω. The enthalpy of ethidium binding was slightly different, -14 kcal/mol for the low ratio data and -12 kcal/mol for the high ratio data. The equilibrium constant at 25°C was 25 x 10^5 M^{-1} in both cases. The χ^2 for both sets were about 1.9 x 10^{-4}. As before, we have assumed that the cooperativity is manifested totally in a change of entropy for the adjacent binding site. Since the reduced chi-squared of both the strong terminal binding site and the cooperative binding model were similar, we cannot distinguish which model is better from these data. Both models fit the data equally well.

We also tested a model which assumes that the ethidium binds more strongly to the one pyrimidine-purine site, $\overset{C-A}{\underset{G-U}{\cdot\,\cdot}}$, than to the purine-purine sites, $\overset{A-A}{\underset{U-U}{\cdot\,\cdot}}$ and $\overset{A-G}{\underset{U-C}{\cdot\,\cdot}}$. This model clearly did not fit the data at high ethidium:strand ratios. This is surprising, considering the well-known preference of ethidium to bind to pyrimidine-purine sites.

BINDING OF ETHIDIUM TO dCA_5G + dCT_5G

The spectral effects of ethidium binding to the deoxyribo-oligonucleotides are similar to those of the ribo-oligonucleotides.

Figure 5 shows the melting curves at 260 and 283 nm, respectively, of dCA_5G + dCT_5G + ethidium at a strand concentration of about 40μM, with ethidium:strand ratios of about 0.4, 0.6, and 0.8.

The melting curves at 283 nm do not level off at low temperatures, which indicates that ethidium does not bind as strongly to the deoxyribo-

oligonucleotides as it does to the ribo-oligonucleotides. This makes it much more difficult to determine the extinction coefficient for the bound ethidium, since all of the ethidium is not bound at 0°C. The values of the extinction coefficients for bound ethidium at 260 and 283 nm were determined by an iterative process whereby a value was estimated, and the fraction double strands and ethidium bound were calculated. This was fit to the model, and the calculated and measured curves of the fraction of ethidium bound were compared. The values for the extinction coefficients were varied until the agreement was good. This procedure to determine extinction coefficients is not as direct as that used for the ribo-oligonucleotides and could potentially bias the results to fit the model (see Discussion). The resulting extinction coefficients of bound ethidium are $\varepsilon_{260} = 1.4 \times 10^4 - 15(T)$ and $\varepsilon_{283} = 2.2 \times 10^4 + 75(T)$, and are included in Table II.

Figure 6 shows the fraction double-strands and fraction ethidium bound at an ethidium:strand ratio of 0.8. Comparing this with Figure 3, it is clear that ethidium binding does not stabilize the double strands of the deoxyribo-oligonucleotides nearly as much as it stabilizes the ribo-oligonucleotides. The double strands formed by these deoxyribo-oligonucleotides are more stable than the ribo-oligonucleotides (18), so this weaker binding of ethidium to the deoxyribo-oligonucleotides is associated with a greater stability of the double strands.

Because the binding of ethidium was weaker for the deoxyribo- than for ribo-oligonucleotides, we were constrained to work at high strand concentration, and low ethidium:strand ratios, as explained above. The values used for the thermodynamics of double-strand formation were $\Delta H_h^\circ = -50$ kcal/mol and $\Delta S_h^\circ = -148$ e.u. (18).

We tested the same two models as were used in the ribo-oligonucleotides, however, the best fits were found to be either with $\tau = 1$ for the strong terminal binding sites model, or $\omega = 1$ for the cooperativity model. The resulting thermodynamic parameters for ethidium binding were found to be $\Delta H_d^\circ = -9$ kcal/mol, $\Delta H_d^\circ = -10$ e.u., and $K_d(25°C) = 0.25 \times 10^5$, with $\chi^2 = 0.4 \times 10^{-4}$ (see Table III). Because of the limitations of determining the extinction coefficients of the bound ethidium, the fit to the model must be considered with more caution. However, the results clearly indicate that the binding to the deoxyribo-oligonucleotides is quite different than to the ribo-oligonucleotides. The effect of errors on the thermodynamics of double-strand formation is comparable to the previous case.

DISCUSSION

In the models presented here, the assumption was made that ethidium ion binds only to double helices by intercalation. It is well known that the binding of ethidium to single strands is very much weaker than binding to double strands. Ethidium binding studies on homopolymers showed very clearly the dramatic increase in ethidium binding to the double-stranded poly(A)•poly(U) relative to the binding to either single-stranded poly(A) or poly(U) (4). The same result was obtained for the deoxyribo-dinucleoside phosphates dCpA and dTpG, wherein binding of the ethidium ion as measured by fluorescence increased greatly when the non-selfcomplementary dinucleoside phosphates were mixed, relative to the separate dinucleoside phosphates (7).

In studies on the binding of ethidium ion to the tetranucleotide dC-G-C-G, Kastrup et al. (26) determined from circular dichroism measurements that two ethidium ions can bind to the ends of the double helices. This binding was much weaker than intercalation, and occurred to a significant degree only if the ratio of ethidium:strand became large. Since the ethidium:strand ratio

for all of the melting curves analyzed in the present study were always 3 or less, outside binding probably contributes very little to the binding of ethidium. Further justification is seen in Figure 4, where three ethidium ions clearly bind when an excess of ethidium is present.

The assumption that the extinction coefficient of the bound ethidium does not depend on which site is filled, and that two ethidium ions bound to a double strand absorb twice as much as one ethidium bound, are more difficult to verify. However, these assumptions allowed a very good fit to all the data.

COMPARISON OF ETHIDIUM BINDING TO $rCA_5G + rCU_5G$ AND $dCA_5G + dCT_5G$

Table III summarizes the results for both the ribo-oligonucleotides and the deoxyribo-oligonucleotides. A maximum of three ethidiums are bound. For the deoxyribo-oligonucleotides, the only model that fit the data well had all the binding sites of equal strength, with no cooperativity between binding sites. For the ribo-oligonucleotides, the sites were strongly unequivalent. Two models fit the data equally well: either the two terminal binding sites were both stronger than the interior binding sites by a factor of about 140, or all the binding sites were of equal strength, but there was anticooperativity between the binding sites with $\omega = 0.1$. The binding of ethidium ion to the ribo-oligonucleotide is about an order of magnitude stronger than it is to the deoxyribo-oligonucleotide.

A possible explanation for the large difference in the way that ethidium binds to RNA compared to DNA is that RNA double helices are more rigid than DNA double helices. X-ray crystalography studies on ethidium complexes with iodoUpA and iodoCpG showed that the iodoU and iodoC sugars have C3' endo conformations, whereas the A and G sugars have C2' endo conformations (27,28). From this, the authors proposed a general model for ethidium binding

wherein the sugar conformations become C3' endo - ethidium - C2' endo. DNA B-form has a C2' endo sugar conformation, whereas RNA A-form has a C3' endo conformation. DNA can assume a number of different conformations with changing solvent conditions such as high salt concentrations, ethanol, etc., whereas RNA structure remains predominately A-form regardless of the solvent conditions. Thus, the DNA may be better able to adjust the sugar conformation on the 5' side of the bound ethidium to C3' endo, whereas the RNA cannot adjust the sugar on the 3' side of the bound ethidium to C2' endo as readily. Thus, ethidium binds without cooperativity to the DNA double helices, but the rigidity of the RNA double helix is large enough to cause cooperativity.

COMPARISONS WITH PREVIOUS RESULTS

Previous studies of ethidium bromide intercalation into nucleic acids have generally been carried out on polynucleotides or dinucleotides by monitoring the absorbance or fluorescence of ethidium at visible wavelengths near 480 nm, or by NMR techniques.

Experiments of ethidium bromide binding to dinucleotides and dinucleoside phosphates have shown quite clearly that ethidium binds preferentially to pyrimidine-purine sequences compared to purine-purine and purine-pyrimidine sequences (7,10,11,12). For example, the complex rUpA-rUpA-ethidium is about 14 times stronger at 0°C than the complex rApU-rApU-ethidium (12). However, comparisons of the strength of ethidium binding to different sequences is complicated by the fact that the dinucleoside phosphates form very unstable double strands in the absence of ethidium, making the determination of the equilibrium constant for double strand formation difficult (13,14). Also, dinucleotide studies cannot measure cooperative effects, since there is only one binding site. Further verification of the pyrimidine-purine preference

was obtained by studies on the tetranucleotides dC-G-C-G, dG-C-G-C, dC-C-G-G and dG-G-C-C using optical (26) and NMR (29) techniques.

Based on these earlier findings, we expected that the binding of ethidium to the oligomers in this study would best be fit by a model which assumed that the one pyrimidine-purine site, $\overset{C-A}{G-U}$, would be stronger than the purine-purine sites, $\overset{A-A}{U-U}$ and $\overset{A-G}{U-C}$. However, this model was clearly inconsistent with the data for the ribo-oligonucleotides $rCA_5G + rCU_5G$; two sites had a stronger binding, not one. Testing this model with the deoxyribo-oligonucleotides $dCA_5G + dCT_5G$ resulted in the best fit with the pyrimidine-purine site being approximately equal to the other. Thus, these deoxyribo-oligonucleotides did not show a great sequence effect. Of course, these oligonucleotides contain no purine-pyrimidine sites, and hence we cannot compare pyrimidine-purine and purine-pyrimidine sites in this study.

In order to explain the binding of ethidium bromide to DNA polymers, statistical models have been developed which take nearest-neighbor exclusion into account (30). The theory of McGhee and von Hippel (31) also takes cooperativity between the binding sites into account.

The binding of ethidium bromide to calf thymus DNA in 1M NaCl was found to fit very well to the model of nearest-neighbor exclusion and no cooperativity, with a binding constant at 19°C of $1.8 \times 10^4\ M^{-1}$ (9). This binding constant is an average for all the different binding sites in DNA. Also, at the higher salt concentration, ethidium binding is weaker than at 0.2M NaCl. However, their results on DNA compares well with the value determined in this study, $3.5 \times 10^4\ M^{-1}$ at 19°C and 0.2M NaCl.

The enthalpy of ethidium bromide binding to calf thymus DNA has been measured by batch and flow microcalorimetry (32). The enthalpy they measured for ethidium binding to DNA in 0.1M KCl at 25°C was -6.7 kcal/mol. The

enthalpy was 0.5 kcal/mol more positive in 0.015M salt concentration. This corresponds well with the value measured in this study for the enthalpy of ethidium binding to the deoxyribo-oligonucleotides, -9 kcal/mol in 0.2M salt.

The data on ethidium bromide binding to RNA are more limited by the unavailability of RNA's which are double-stranded. Douthart et al. (33) studied ethidium binding to the double-stranded RNA obtained from the mycophage Penicillium chrysogenum. From Scatchard plots at different salt concentrations, they determined that the saturation binding occurred at r = 0.38 ethidium ions bound/base pair in 0.1M sodium cacodylate, 0.32 in 0.01M sodium cacodylate, and 0.18 in 0.001M sodium cacodylate. The binding constant from the slope and the intercept of the Scatchard plot was found to be 4.7×10^6 M^{-1} at 25°C and in 0.1M NaCl. Thus, the binding constant for ethidium bromide is much larger for RNA than for DNA.

The Scatchard analysis used by Douthart et al. (33) assumes the binding sites are equal and independent. However, their data could also be analyzed using a McGhee-von Hippel analysis (31), assuming nearest-neighbor exclusion and cooperativity. It is impractical to analyze their data quantitatively, but qualitatively their data can be fit using their equilibrium constant, with a cooperativity parameter of about 0.4 or 0.5 (19).

In conclusion, this study utilized oligonucleotides and a statistical model to probe the interaction of nucleic acids with ethidium ions in order to determine quantitatively the sequence dependence of ethidium binding and the differences between DNA and RNA. The techniques developed here can be applied to a number of oligonucleotide sequences in order to better quantitate the sequence specificity of ethidium binding, and to determine what factors are important in the stabilization of the intercalation complex. The most interesting new finding was the large difference in site specificity for

binding to DNA and RNA oligonucleotides of equivalent sequence. For RNA the terminal $\overset{C-A}{\underset{G-U}{:\ :}}$ and $\overset{A-G}{\underset{U-C}{:\ :}}$ sites bound ethidium two orders of magnitude more strongly than the internal $\overset{A-A}{\underset{U-U}{:\ :}}$ sites. For DNA the terminal $\overset{C-A}{\underset{G-T}{:\ :}}$ and $\overset{A-G}{\underset{T-C}{:\ :}}$, and internal $\overset{A-A}{\underset{T-T}{:\ :}}$ sites all bound ethidium with the same intrinsic equilibrium constant.

We are grateful to Dr. Francis H. Martin for the synthesis of these oligonucleotides and for help in the early stages of this work. The research was supported in part by National Institutes Health Grant GM 10840 and the U. S. Department of Energy, Office of Energy Research, under Contract No. 03-82ER60090.000. and Contract No. DE-AC03-76SF00098.

REFERENCES

1. Streisinger, G., Okada, Y., Emrich, J., Newton, J., Tsugita, A., Terzaghi, E. & Inouye, M. (1966) Cold Spring Harbor Symp. Quant. Biol. 31, 77-84.
2. McCann, J., Choi, E., Yamasaki, E. & Ames, B. N. (1975) Proc. Nat. Acad. Sci. 72, 5135-5139.
3. Waring, M. J. (1965) J. Mol. Biol. 13, 269-282.
4. Waring, M. J. (1966) Biochim. Biophys. Acta 114, 234-244.
5. LePecq, J.-B. & Paoletti, C. (1967) J. Mol. Biol. 27, 87-106.
6. Thomas, G. & Roques, B. (1972) FEBS Letters 26, 169-175.
7. Reinhardt, C. G. & Krugh, T. R. (1978) Biochemistry 17, 4845-4854.
8. Kreishman, G. P, & Chan, S. I. (1971) J. Mol. Biol. 61, 45-58.
9. Bresloff, J. & Crothers, D. M. (1975) J. Mol. Biol. 95, 103-123.
10. Krugh, T. R. & Reinhardt, C. G. (1975) J. Mol. Biol. 97, 133-162.
11. Krugh, T. R., Wittlin, F. N. & Cramer, S. P. (1975) Biopolymers 14, 197-210.
12. Dahl, K. S., Pardi, A. & Tinoco, I., Jr. (1982) Biochemistry 21, 2730-2737.
13. Young, M. A. & Krugh, T. R. (1975) Biochemistry 14, 4841-4847.
14. Krugh, T. R., Laing, J. W. & Young, M. A. (1976) Biochemistry 15, 1224-1228.
15. Lee, C.-H. & Tinoco, I., Jr. (1978) Nature 274, 609-610.
16. Pardi, A. (1980) Ph.D. Thesis, University of California, Berkeley, California.
17. Helfgott, D. C. & Kallenback, N. R. (1979) Nucleic Acids Res. 7, 1011-1017.

18. Nelson, J. W., Martin, F. H. & Tinoco, I., Jr. (1981) Biopolymers 20, 2509-2531.

19. Nelson, J. W. (1982) Ph.D. Thesis, University of California, Berkeley, California.

20. Nelson, J. W. & Tinoco, I., Jr. (1982) Biochemistry, 21, 5289-5295.

21. Bevington, P. R. (1969) Data Reduction and Error Analysis for the Physical Sciences, McGraw-Hill, New York, chapter 6.

22. LePecq, J.-B. (1972) Methods of Biochemical Analysis 20, 41-86.

23. Wakelin, L. P. G. & Waring, M. J. (1974) Mol. Pharmacol. 9, 544-561.

24. Breslauer, K. J., Sturtevant, J. M. & Tinoco, I., Jr. (1975) J. Mol. Biol. 99, 549-565.

25. Albergo, D. D., Marky, L. A., Breslauer, K. J. & Turner, D. H. (1981) Biochemistry 20, 1409-1413.

26. Kastrup, R. V., Young, M. A. & Krugh, T. R. (1978) Biochemistry 17, 4855-4865.

27. Tsai, C.-C., Jain, S. C. & Sobell, H. M. (1977) J. Mol. Biol. 114, 301-315.

28. Jain, S. C., Tsai, C.-C. & Sobell, H. M. (1977) J. Mol. Biol. 114, 317-331.

29. Patel, D. J. & Canuel, L. L. (1979) Eur. J. Biochem. 96, 267-276.

30. Crothers, D. M. (1968) Biopolymers 6, 575-584.

31. McGhee, J. D. & von Hippel, P. H. (1974) J. Mol. Biol. 86, 469-489.

32. Quadrifoglio, F., Crescenzi, V. & Giancotti, V. (1974) Biophysical Chemistry 1, 319-324.

33. Douthart, R. J., Burnett, J. P., Weasley, F. W., & Frank, B. H. (1973) Biochemistry 12, 214-220.

TABLE I

Statistical Weights of Double Helices

with Ethidium Ions Bound

no. of ethidium ions bound (i)	no. of terminal sites filled	statistical weight*	no. of species	g_i
0	0	K_h	1	1
1	0	$K_h S$	4	$2\tau + 4$
	1	$\tau K_h S$	2	
2	0	$K_h S^2$	3	$\tau^2 + 6\tau + 3$
	1	$\tau K_h S^2$	6	
	2	$\tau^2 K_h S^2$	1	
3	0	$K_h S^3$	0	$2\tau^2 + 2\tau$
	1	$\tau K_h S^3$	2	
	2	$\tau^2 K_h S^3$	2	

* Statistical weight of single strands = 1. $S = C_f K_d$.

TABLE II

Extinction Coefficients at 260 and 283 nm
in 0.2M NaCl, 0.01M Phosphate Buffer, pH=7, 0.1mM EDTA[a]

Ethidium bromide:

$\varepsilon_{260} = 1.7 \times 10^4 - 25.5(T - 50)$

$\varepsilon_{283} = 5.1 \times 10^4 - 74(T - 90) + [0.25\sqrt{\text{concentration}} + 4.4 \times 10^{-4}](T-90)^3$

---

rCA_5G + rCU_5G single strands:

$\varepsilon_{260} = 1.40 \times 10^5 + 190(T-50) - 2.35(T-50)^2 - 0.0237(T-50)^3$

$\varepsilon_{283} = 4.17 \times 10^4 - 10.4(T - 50)$

rCA_5G + rCU_5G double strands:

$\varepsilon_{260} = 1.14 \times 10^{5*} + 240(T)$

$\varepsilon_{283} = 4.21 \times 10^4$

Ethidium bromide bound to $rCA_5G \cdot rCU_5G$

$\varepsilon_{260} = 9.1 \times 10^3 - 15(T)$

$\varepsilon_{283} = 2.0 \times 10^{4*} + 50(T)$

---

dCA_5G + dCT_5G single strands:

$\varepsilon_{260} = 1.41 \times 10^5 + 170(T - 50)$

$\varepsilon_{283} = 5.4 \times 10^4 + 40(T - 50)$

dCA_5G + dCT_5G double strands:

$\varepsilon_{260} = 1.14 \times 10^5 + 150(T)$

$\varepsilon_{283} = 5.25 \times 10^4$

Ethidium bromide bound to dCA_5G + dCT_5G:

$\varepsilon_{260} = 1.4 \times 10^4 - 15(T)$

$\varepsilon_{283} = 2.2 \times 10^4 + 75(T)$

---

[a]Temperatures are in °C.

*Value varies slightly with concentration of strands.

TABLE III

Thermodynamics of Ethidium Ion Binding to

$rCA_5G + rCU_5G$ and $dCA_5G + dCT_5G$, 0.2M NaCl

Oligomers	Model	$\Delta H°$ (kcal/mol)	$\Delta S°$ (e.u.)	K_d(25°C) (x 10^{-5} M^{-1})
$rCA_5G + rCU_5G$	Two strong terminal sites, τ = 140	-14±4	-21±9	(strong) 6±1 (weak) 0.04±0.01
$rCA_5G + rCU_5G$	Cooperativity, ω = 0.1	-14±4	-22±9	2.5±0.4
$dCA_5G + dCT_5G$	All sites equal	-9±3	-10±7	0.25±0.04

FIGURE LEGENDS

Figure 1. Absorbance of ethidium bromide *vs.* temperature in 0.2M NaCl, 0.01M phosphate buffer, pH = 7, 0.01mM EDTA. The curves are normalized by dividing by the absorbance at 90°C. Hence the parameter plotted is $\varepsilon_{283}(T)/\varepsilon_{283}(90°C)$. The lines show the fit using the equation $\varepsilon_{283}(T)/\varepsilon_{283}(90°C) = 1 - 1.45 \times 10^{3}\ (T - 90°C) + (4.9 \times 10^{-6} \sqrt{\text{concentration}} + 8.6 \times 10^{-9})\ (T - 90°C)^{3}$.

Figure 2. (a) Melting curves at 260 nm of rCA_5G + rCU_5G + ethidium, for the concentration of strands roughly equal and the ratio of ethidium:strands varied. The data are all normalized at 60°C. The concentrations of ethidium:strands were (μM): 0:62; 4.4:52; 9.4:51; 25:50; 50:49; 106:50; and 156:49. (b) Melting curves at 283 nm.

Figure 3. The fraction double strands formed by rCA_5G + rCU_5G alone (□), the fraction double strands in a mixture of strands and ethidium (○), and the fraction ethidium bound in the mixture (◇). The concentration of strands alone was 62μM. The concentration of strands in the mixture was 49μM, the concentration of ethidium was 50μM.

Figure 4. The number of ethidium ions bound at a roughly constant strand concentration of 49-53μM at ethidium:strand ratios of (a) 0.50; (b) 1.04; (c) 2.12; (d) 3.16; and (e) 4.18. The lines to the left of the curves indicate the input ethidium:strand ratios.

Figure 5. (a) Melting curves at 260 nm of dCA_5G + dCT_5G + ethidium, holding the concentration of strands roughly equal and changing the ratio of ethidium:strands. The data are all normalized at 50°C. The concentrations of ethidium:strands (μM) were: 0:44; 19:44; 24:42; and 31:40. (b) Melting curves at 283 nm.

Figure 6. The fraction double strands formed by $dCA_5G + dCT_5G$ alone (□), the fraction double strands in a mixture of strands and ethidium (○), and the fraction ethidium bound in the mixture (◇). The concentration of the strands alone was 44μM. The concentration of the strands in the mixture was 40μM; the ethidium concentration in the mixture was 31μM.

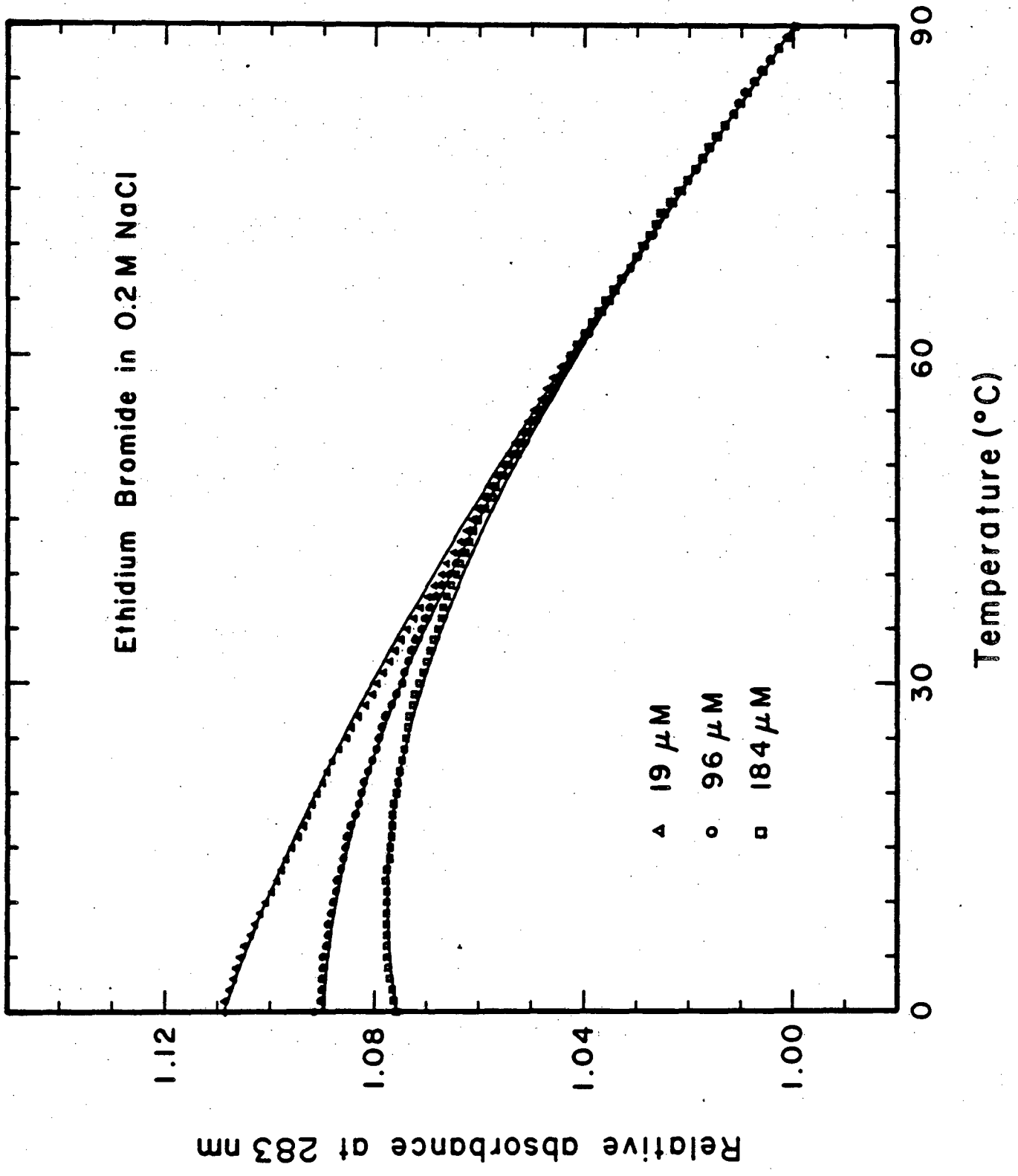
Ethidium Bromide in 0.2 M NaCl
19 μM
96 μM
184 μM
Relative absorbance at 283 nm
1.12
1.08
1.04
1.00
0
30
60
90
Temperature (°C)

Figure 1

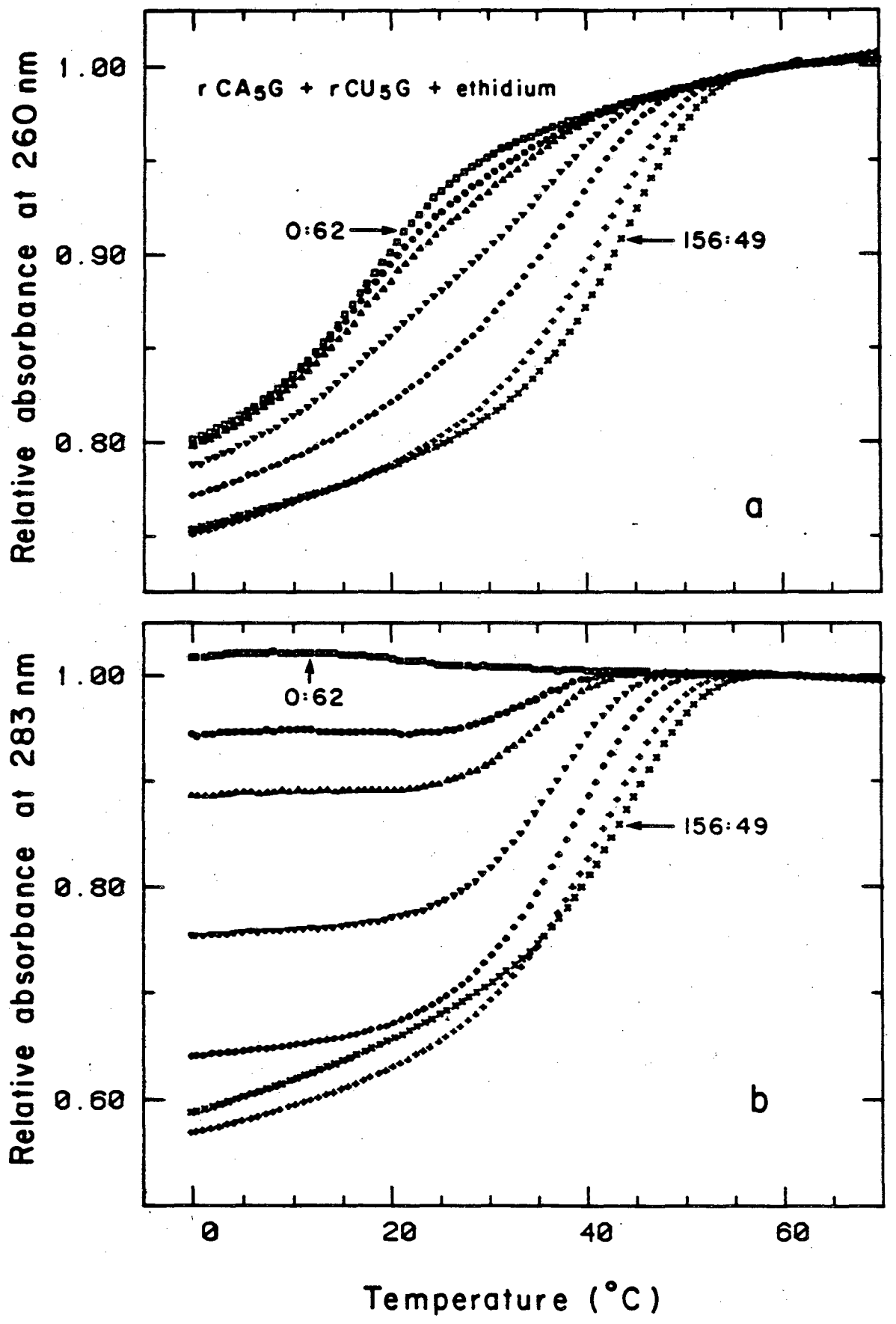
rCA5G + rCU5G + ethidium
0:62
156:49
a
Relative absorbance at 260 nm
1.00
0.90
0.80
0:62
156:49
b
Relative absorbance at 283 nm
1.00
0.80
0.60
0
20
40
60
Temperature (°C)

Figure 2

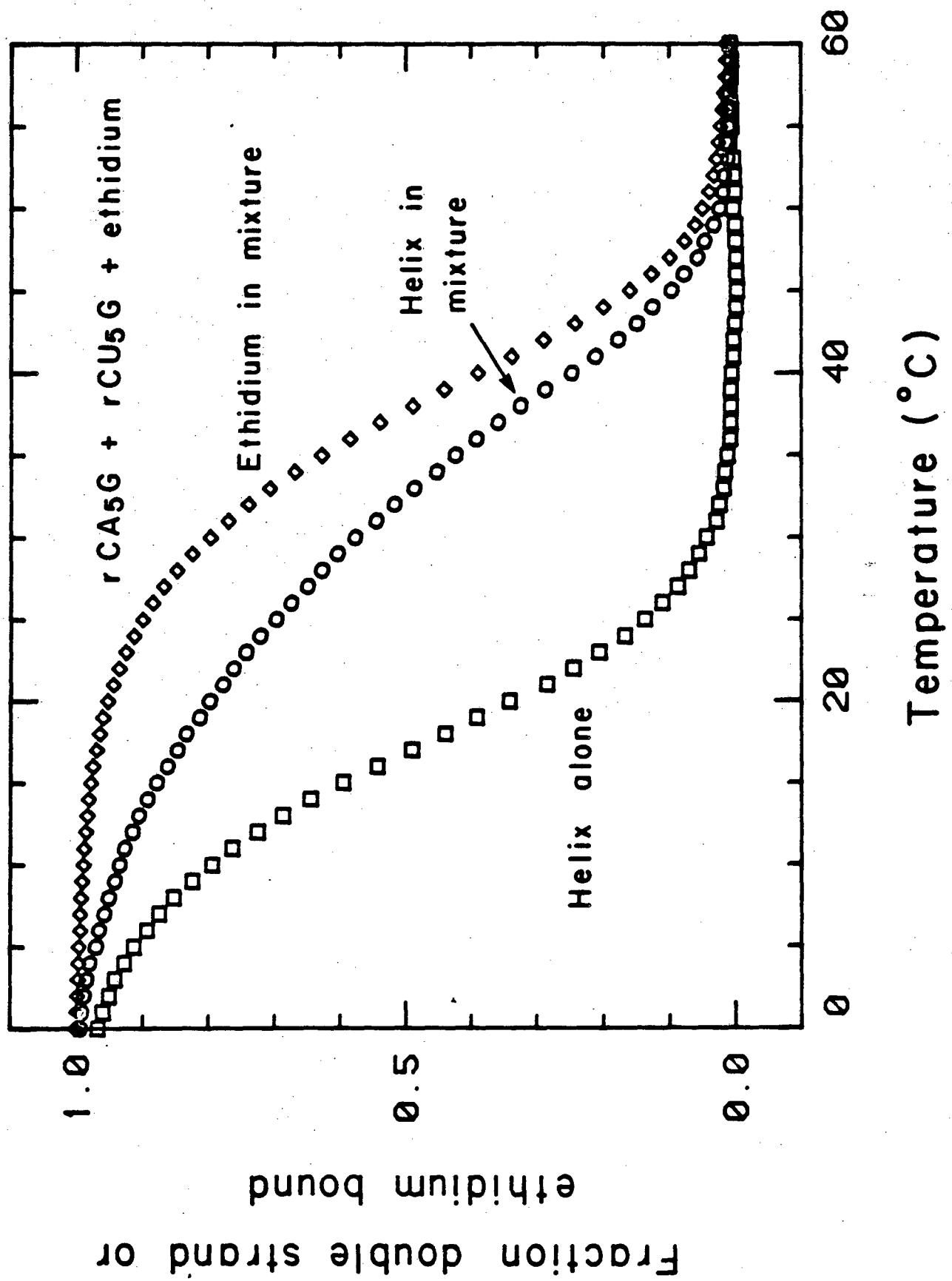
rCA5G + rCU5G + ethidium
Ethidium in mixture
Helix in mixture
Helix alone
1.0
0.5
0.0
0
20
40
60
Temperature (°C)
Fraction double strand or ethidium bound

Figure 3

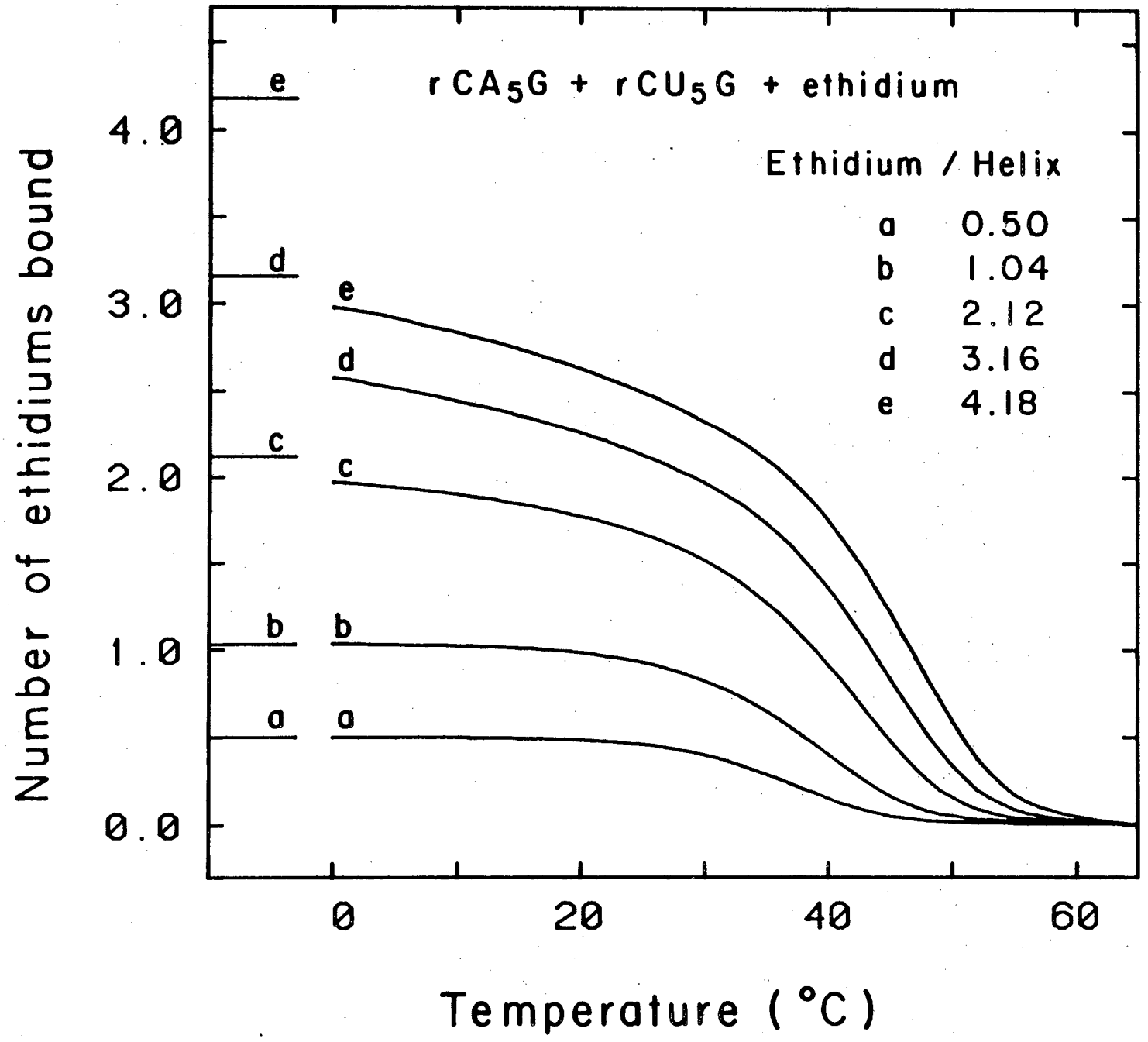
rCA5G + rCU5G + ethidium
Ethidium / Helix
a 0.50
b 1.04
c 2.12
d 3.16
e 4.18
Number of ethidiums bound
4.0
3.0
2.0
1.0
0.0
0
20
40
60
Temperature (°C)

Figure 4

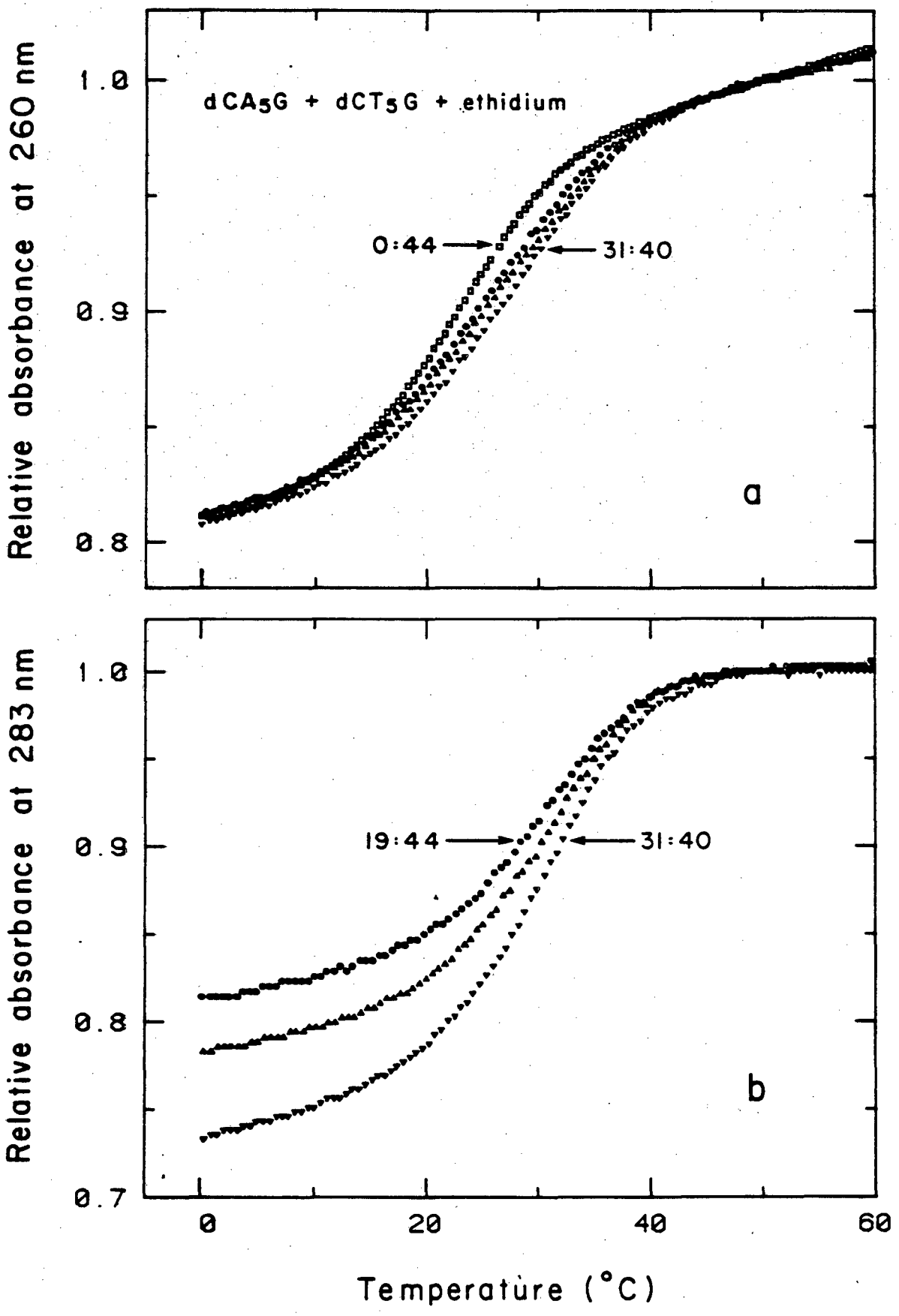
dCA5G + dCT5G + ethidium
0:44
31:40
a
Relative absorbance at 260 nm
1.0
0.9
0.8
19:44
31:40
b
Relative absorbance at 283 nm
1.0
0.9
0.8
0.7
0
20
40
60
Temperature (°C)

Figure 5

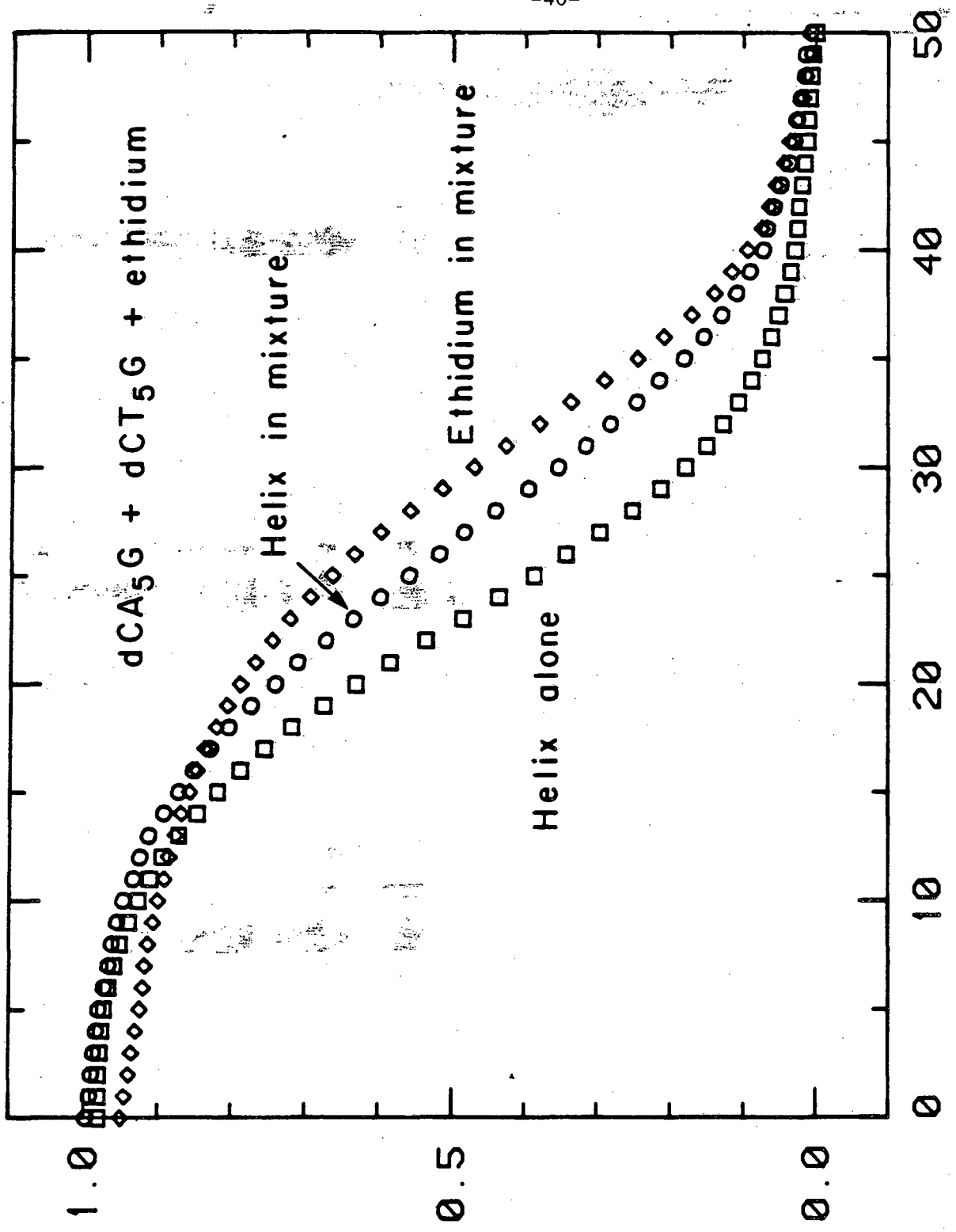
dCA5G + dCT5G + ethidium
Helix in mixture
Ethidium in mixture
Helix alone
Fraction double strand or ethidium bound
1.0
0.5
0.0
0
10
20
30
40
50
Temperature (°C)

Figure 6

TECHNICAL INFORMATION DEPARTMENT
LAWRENCE BERKELEY LABORATORY
UNIVERSITY OF CALIFORNIA
BERKELEY, CALIFORNIA 94720